

SNAPSHOT: SUITE FOR THE NUMERICAL ANALYSIS OF PLANETARY PROTECTION

Francesca Letizia*, Camilla Colombo[†],
Jeroen P.J.P. Van den Eynde[‡], Roberto Armellini[§].

University of Southampton
Astronautics Research Group
Southampton, SO17 1BJ
United Kingdom

Rüdiger Jehn

Mission Analysis
ESOC
Darmstadt, 64293
Germany

ABSTRACT

For interplanetary missions and missions to the Lagrangian points, the compliance with planetary protection requirements should be verified as spacecraft and launchers used for these applications may be inserted in a trajectory that will impact the Earth or other planets. A new tool, SNAPSHOT, was developed for this purpose. A Monte Carlo analysis is performed considering the dispersion of the initial condition and of other parameters such as the area-to-mass ratio. Each run is characterised by studying the close approaches through the b-plane representation to detect conditions of impacts and resonances. The application of the tool to two missions (Solo and BepiColombo) is presented.

Index Terms— planetary protection, Monte Carlo analysis, b-plane

1. INTRODUCTION

Spacecraft and launchers used for interplanetary missions and mission to the Lagrangian points may be inserted into orbits that can come back to the Earth or impact other planets. This has already happened as in the case of the third stage of Apollo 12 that was discovered to be in an orbit that gets temporarily captured by the Earth every 40 years [1]. Recently, the object WT1190F, which is also supposed to belong to a lunar mission, re-entered in the atmosphere [2].

The probability of these events to happen should be estimated during the phase of the design of a mission to ensure it is compliant with planetary protection requirements

*The authors acknowledge the use of the IRIDIS High Performance Computing Facility, and associated support services at the University of Southampton, in the completion of this work.

[†]The present study was funded by the European Space Agency through the contract 4000115299/15/D/MB, *Planetary Protection Compliance Verification Software*.

[‡]Currently Research Fellow, European Space Agency, ESTEC, Noordwijk, 2200AG, The Netherlands.

[§]Currently Marie Curie Research Fellow at Scientific Computing Group (GRUCACI), Universidad de La Rioja, ES-26004 Logroño, Spain

[3]. These requirements are in place to limit the risk of contamination of celestial bodies due to space missions and they prescribe a maximum allowed impact probability that should be verified over a time window of 50-100 years, considering possible inaccuracies of the launcher or failures of the propulsion system.

For this purpose, a new tool, called SNAPSHOT (Suite for the Numerical Analysis of Planetary Protection), was developed by the University of Southampton under a study for the European Space Agency. The tool is based on a Monte Carlo approach to study the dispersion of the initial conditions of launchers or spacecraft. Each trajectory is then analysed with the b-plane representation to identify impacts and resonances with celestial bodies. In the rest of the paper, Section 2 will give an overview of the method and Section 3 will show the application to the launcher of Solo and to BepiColombo.

2. SNAPSHOT

SNAPSHOT is a code written in modern Fortran for the analysis of a mission compliance with planetary protection requirements, based on a Monte Carlo analysis. Figure 1 shows a block diagram of the tool. The first main block is the initialisation of the Monte Carlo (MC) simulation. The user specifies the maximum allowed probability of impact with a specific body and the desired confidence level, together with providing the covariance matrix associated to the initial state and, if necessary, additional distributions such as the one of area-to-mass ratio (A/M). The tool computes the required number of Monte Carlo runs and samples the covariance matrix to obtain the initial conditions. Each initial condition is propagated and then analysed with the representation on the b-plane of the relevant bodies. The number of detected impacts is computed: if the number is not compatible with the requirements, the number of MC runs is increased until the requirements are fulfilled or the maximum number of runs is reached. At the end of the runs, the output is produced and its post-processing is performed in MATLAB.

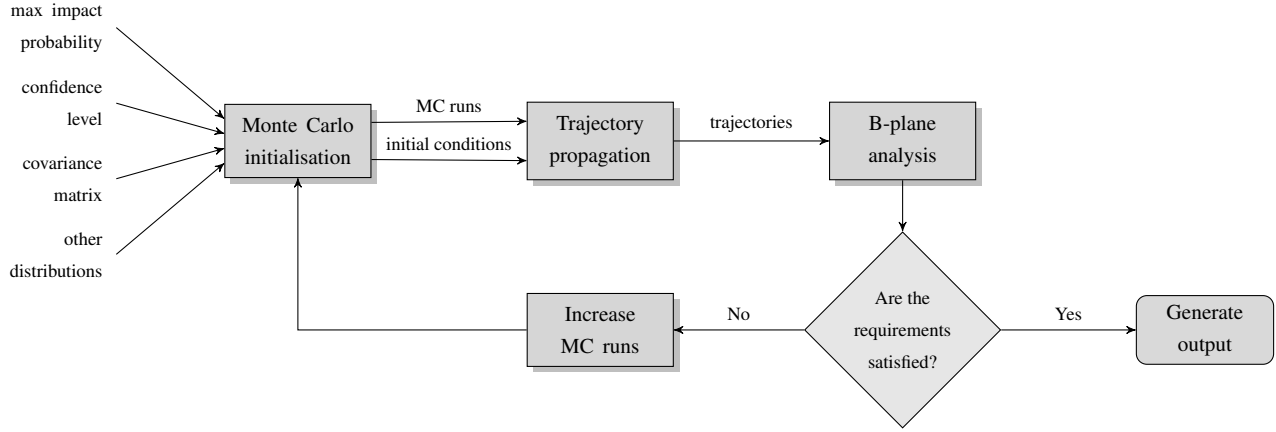


Fig. 1: SNAPSHOT building blocks.

2.1. Monte Carlo samples generation

The number of MC runs necessary to verify the planetary protection requirements is found by applying the expression of Wilson's confidence interval as in Jehn [4] and Wallace [5]. Differently from the latter, the expression for the one-sided interval is used.

The MC runs can be considered as a binomial process with only two possible outcomes, generally labelled as *success* and *failure*, which in the present application correspond to *impact* and *no impact*. In the current implementation, the user is asked to identify a reference body for this evaluation. The selection of a reference body is used only to evaluate if the number of MC runs should be increased, whereas impacts with all considered celestial bodies are registered. In the results in Section 3, Mars is set as the reference body, so only impacts with this planet will trigger the increase of the number required runs. This is done because Mars has more stringent planetary protection requirements than other planets due to possible presence of habitats (or their rest) on its surface.

The output of the MC is considered as a binomial variable $X \sim B(n, p)$, with n number of trials and p the success probability in each trial. The expression of the one-sided Wilson's interval is

$$p \leq \left(\frac{\hat{p} + \frac{z_\alpha^2}{2n} + z_\alpha^2 \sqrt{\frac{\hat{p}(1-\hat{p})}{n} + \frac{z_\alpha^2}{4n^2}}}{1 + \frac{z_\alpha^2}{n}} \right). \quad (1)$$

where \hat{p} is the probability of success estimated from the statistical sample (e.g. $\hat{p} = n_I/n$, with n_I number of impacts), z_α is the α quantile of a standard normal distribution, α is the confidence level [6].

In SNAPSHOT, the user sets the value of the maximum allowed p and the one of α . The corresponding z_α is obtained from a lookup table. At the beginning of the simulation no impacts are recorded, so $\hat{p} = 0$. In this case, Equation 1 can

be easily inverted to find the required number of runs

$$n = \frac{z_\alpha^2(1-p)}{p}. \quad (2)$$

If after n runs the number of impacts is different from zero, Equation 1 should be used again, with the new value of \hat{p} , to update the value of n . Note that when $\hat{p} = 0$, Equation 1 cannot be inverted analytically, so Newton's method is used. Jehn [4] proposed an analytical approximation of $n = n(n_I)$, but this was not applied here because Newton's method has a fast convergence and the time spent in the computation of n is negligible compared to the time used for the propagation of the trajectories. The analysis is terminated when the compliance is demonstrated or the maximum number of runs is reached. This limit is currently set equal to 500000 runs. Alternatively, the user can set the desired number of MC runs.

Once the number of runs is defined (or updated), the corresponding initial conditions need to be generated. When the dispersion of the initial condition is described by a covariance matrix, Cholesky factorisation [7] is used to obtain correlated deviations from random generated numbers. When the case of the failure of the propulsion system is studied, the random generated numbers are used to define the instants of failure and the initial conditions are obtained by linear interpolation of the state vector at the closest times. Additional distributions can be considered such as the one of the area-to-mass ratio. In this case, the user provides the known values (e.g. the minimum, the average and the maximum value) and selects a distribution; currently, the uniform and the triangular distribution are implemented.

2.2. Trajectory propagation

Once the initial state is defined, the trajectory is propagated over 100 years, using Cartesian coordinates in the J2000 reference frame centred in the solar system barycentre. To keep the tool flexible, the initial state of the object can be provided

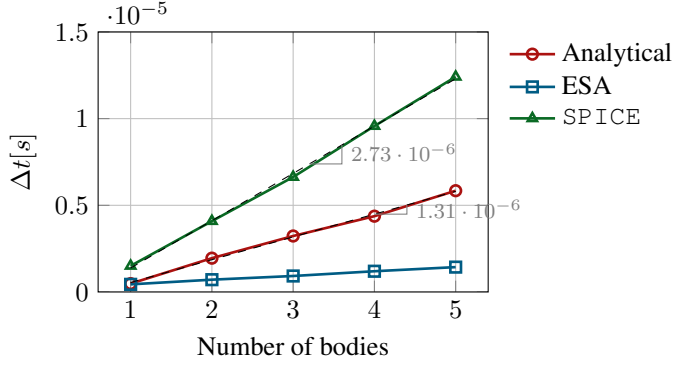


Fig. 2: Timing of the call of the ephemeris routines as a function of the number bodies.

by the user in a reference systems with different orientation (e.g. the ecliptic one) or a different centre (e.g. the Sun). When the results of the MC are shown in functions of the state vector components (as in Section 3), then the body reference is used because this reference frame offers a direct connection to the physics of the evolution of the trajectory.

The integration is carried out in dimensionless variables and the trajectory is propagated under the effect of gravitational forces and the solar radiation pressure; additional forces such as relativistic effects, will be included in the future. For the solar radiation pressure, a simple cannonball model is adopted

$$\ddot{\mathbf{r}} = -C_R \frac{A}{m} \Phi_{\text{ref}} \left(\frac{r_{\text{ref}}}{r_{\text{SC,Sun}}} \right)^2 \frac{\mathbf{r}_{\text{SC,Sun}}}{r_{\text{SC,Sun}}}, \quad (3)$$

where C_R is the reflectivity coefficient, A/m the area-to-mass ratio, Φ the solar radiation pressure at a reference distance r_{ref} from the Sun and $\mathbf{r}_{\text{SC,Sun}}$ the vector between the object and the Sun. For the gravitational forces, the resulting acceleration $\ddot{\mathbf{r}}$ on the launcher is obtained from

$$\ddot{\mathbf{r}} = \sum_j \frac{Gm_j \mathbf{r}_j}{|\mathbf{r}_j|^3}, \quad (4)$$

where G is the gravitational constant, m_j indicate the mass of the celestial body j , \mathbf{r}_j is the distance between the body and the object. The user can select which celestial objects to include in the propagation, among the Sun, the planets, the Moon and Pluto.

Three possible options for the ephemerides are included in SNAPSHOT and the computational time associated to their calls is shown in Figure 2. The computational time of ephemeris routines is crucial as it is one of the most expensive operations in the simulations performed in SNAPSHOT; for the propagation of trajectories as the ones shown in Section 3, the ephemeris routine is responsible for around 60% of the run time. The first option is the use of analytical planetary ephemerides by Dysli [8]. These ephemerides are

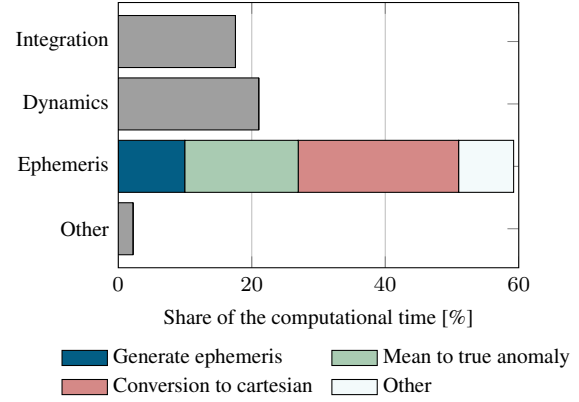


Fig. 3: Example of computational time break-down for the integration of a trajectory using the analytical ephemerides.

expressed in terms of orbital parameters, so they are not directly suitable for the current application. In fact, the saving in the computational time associated with the analytical formulation vanishes because of the need of conversion to Cartesian coordinates (Figure 3). The other options are the use of ESA routine for planetary ephemerides, based on JPL DE422 file, or the use of JPL SPICE toolkit¹. The two approaches, ESA planetary ephemeris routine and SPICE, and their integration in SNAPSHOT were validated through the comparison with the ephemerides available on the Horizons platform² for different objects (e.g. Apophis, New Horizon, Herschel). The comparison between the two approaches highlighted that the ESA planetary ephemeris routine runs faster than SPICE toolkit, with a computational time lower than one fifth of the one with SPICE for the studied cases. The bottleneck in SPICE run time appears to be connected to the repetitive reading of the binary kernel where the data on the ephemerides is stored. For this reason, the attempt to speed-up SPICE by using low level functions (e.g. with restricted options in terms of the reference system) resulted only in a marginal improvement, with a reduction of the computational time around 12%, so still far from the performance of ESA planetary ephemeris routine. In addition, ESA planetary ephemeris routine allows a thread-safe implementation, such that shared memory parallel programming (e.g. OpenMP) can be used. Even if parallel programming has not been implemented yet in the current version of SNAPSHOT, future work aims to perform the MC runs taking advantages of this possibility.

The trajectories are integrated with Runge-Kutta methods and two possible step size control techniques are implemented. The first one is the classical adaptive step-size technique developed by Dormand and Prince [9]. Within this class, the propagators RK4(3), RK5(4) and RK8(7) are currently implemented. SNAPSHOT is implemented in such

¹Available at <http://naif.jpl.nasa.gov/naif/toolkit.html>.

²Available at <http://ssd.jpl.nasa.gov/horizons.cgi>.

a way that additional Runge-Kutta integrators can be easily added by only providing the corresponding values of their Butcher tableau because a general function is used for all the Runge-Kutta routines.

The other step-size control technique is the one of the *regularised* steps by Debatin et al. [10]. They observed that, in the case of close approaches, the gravitational pull from the planet can be considered as a quasi-impulsive force. If the prescribed integration step, as obtained from the estimation of the truncation error, is too large, the effect of the close approach may be missed. With the regularised step control technique this is avoided by relating the step size to the gravitation component of the force acting on the object. The scaling factor for the step is obtained from the maximum eigenvalue Λ of the Jacobian of the dynamics (considering only the effect of gravitational forces) and Debatin et al. [10] provide an analytical approximation for it

$$\Lambda = \left[\sum_{j=0}^N \frac{2\mu_j}{|x - x_j(t)|^3} \right]^{\frac{1}{2}} \quad (5)$$

where μ_j is the gravitational constant of the j -th considered body. During the integration, the step is rescaled as

$$h_{n+1} = h_n \frac{\Lambda(t_n)}{\Lambda(t_{n+1})}. \quad (6)$$

To initialise the method and have a reference on its accuracy level, the first step of integration is performed using the adaptive step-size control technique, using a propagator with the same order as the one where the *regularised* steps are applied. For this reason, the *regularised*-step technique was adopted for the propagators RK4, RK5 and RK8. Also in this case an extensive comparison was performed, finding that the classical adaptive technique presents the shortest computational time and no issues in dealing with close approaches.

In addition to the implementation of the Runge-Kutta method, the propagator in SNAPSHOT includes two features. The first one is the ability of obtaining the value of the state vector on a finer time grid than the one used for the propagation (*dense output*). This is achieved by using a continuous Runge-Kutta formulation for the adaptive method RK5(4) [11] and a Hermit cubic interpolation for the other cases [12]. Future work will implement a continuous Runge-Kutta formulation also for the RK8(7). The second feature is the possibility for the user to provide *event* functions, i.e. conditions that trigger the stop of the propagation or the saving of the state vector. For example, event functions are used in the current application to halt the propagation when the object is colliding with a planet (i.e. distance from the planet smaller than the radius of the planet). The event function can depend on a combination of values of the state vector (as in the case of the distance) and a defined threshold value (e.g. the radius of the planet). The user can decide if the *event*

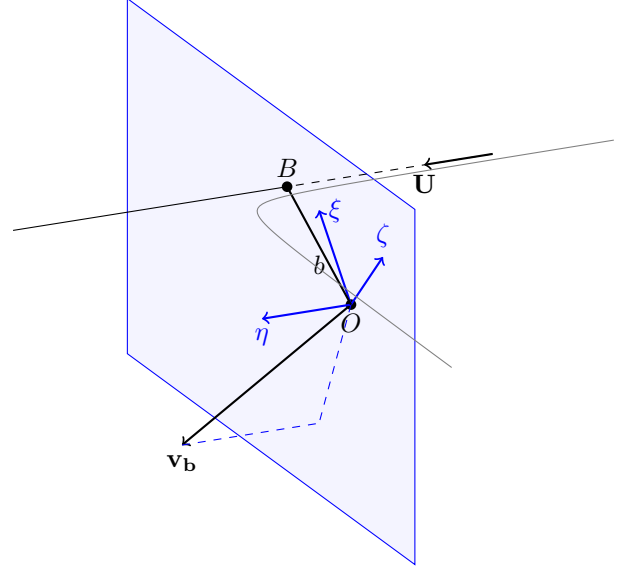


Fig. 4: B-plane definition (in blue). In grey the trajectory of the object at the close approach. \mathbf{U} is the object planetocentric velocity.

should be registered whether the threshold is reached from larger or smaller values or any case. The user can also decide if the condition when the *event* happens needs to be precisely identified: this option, not used at the moment, will be useful in the future to trigger the analysis of a close-approach on the b-plane, described in Section 2.3, directly at the entrance of the sphere of influence and not in post-processing as in the current implementation.

2.3. B-plane analysis

Once the trajectory of the studied object is propagated, the characteristics of the close approaches, if any, are analysed through the representation on the b-plane. A close approach is detected when the distance of the object from any celestial body is lower than the radius of the sphere of influence of the body. The radius of the sphere of influence ($R_{SOI,j}$) of the body j is defined as

$$R_{SOI,j} = \bar{a}_j \left(\frac{\mu_j}{\mu_{ref}} \right)^{\frac{2}{5}} \quad (7)$$

where \bar{a}_j is the mean value of the semi-major axis, μ_j is the gravitational constant of the body, μ_{ref} the one of the reference body, which is the Sun when j refers to the planets and Pluto, and it is the Earth when j refers to the Moon. When the distance from a body j becomes lower than $R_{SOI,j}$, the object trajectory starts to be represented on the b-plane of the body. The b-plane is defined as the plane perpendicular to the object planetocentric velocity \mathbf{U} (Figure 4). The following reference

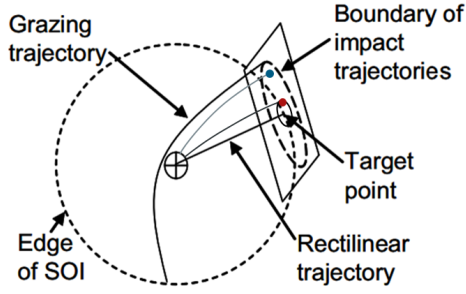


Fig. 5: Definition of the impact region. SOI indicates the Sphere Of Influence. Figure re-adapted from Davis et al. [13].

system is defined [14]:

$$\hat{\eta} = \frac{\mathbf{U}}{\|\mathbf{U}\|} \quad \hat{\xi} = \frac{\mathbf{v}_b \times \hat{\eta}}{\|\mathbf{v}_b \times \hat{\eta}\|} \quad \hat{\zeta} = \hat{\xi} \times \hat{\eta} \quad (8)$$

where \mathbf{U} is the relative velocity of the object with respect with the celestial body, and \mathbf{v}_b is the body velocity around the Sun. The coordinate $\hat{\eta}$ is parallel to the planetocentric velocity \mathbf{U} ; $\hat{\zeta}$ is parallel to the projection of the velocity of the body v_b in the b-plane, but with opposite direction; $\hat{\xi}$ completes the positive reference system. The point B is obtained as the intersection of the incoming asymptote and the b-plane and its distance, b , from the centre is called *impact parameter*.

An impact is detected when the impact parameter is smaller than the radius of the planet: this case is indicated by the red dot in Figure 5. In the same figure, also the blue point result into an impact as it is within the *impact region* defined by the grazing trajectories to the planet. Besides the detection of impacts, the b-plane offers additional information as it allows the separation of the effect of the distance and of the phasing in the analysis of the close approach.

For example, Figure 6 shows the b-plane for the close encounter of Apophis with the Earth in 2029. In this case, the point of close encounter has a large value of the ζ coordinate meaning that the impact does not occur because of the phasing between the Earth and Apophis. On the other hand, a large value of ξ would indicate a large geometrical distance between the two orbits. Therefore, the representation of the close approaches on the b-plane offers a deeper characterisation of the close approach than the study of the miss distance only.

Another state that can be represented on the b-plane is the resonance between the object and a celestial body. Thanks to the analytical theory by Valsecchi et al. [15], these conditions can be represented on the b-plane as circles (Figure 6), whose radius and centre depends on the geometry of the close approach and on the value of the resonance. Beside the detection of impacts, SNAPPSHOT also identifies conditions of resonances and these states are used to characterise the single MC run.

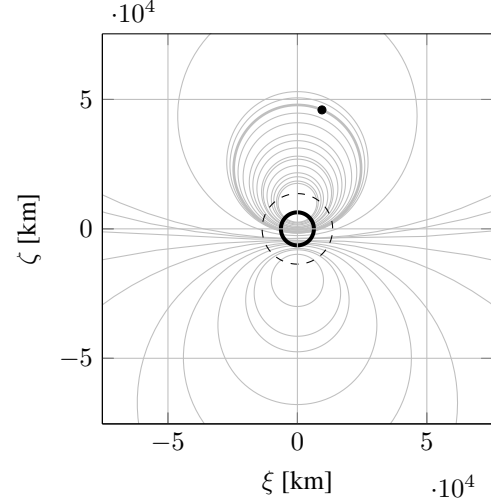


Fig. 6: Representation of the close approach of Apophis with the Earth on the b-plane. The thick black line represents the radius of the Earth, the dashed line the radius of the impact region and the grey circles the conditions of resonances.

Even if multiple close approaches may be recorded in a single trajectory, only one state should be selected to characterise the trajectory. Two options are currently implemented in the tool: the choice of the condition at the first close approach or the one at the *worst* encounter. The first option was motivated by the fact that the first close encounter is also the one with the lowest uncertainty and the detection of resonances can be used to estimate the probability of impacts in the future. However, when the compliance with planetary protection requirements should be verified, it becomes essential to perform the numerical propagation for the whole prescribed time window. As a consequence, the conditions to identify the *worst* close encounter should be defined. Also in this case two options are considered in SNAPPSHOT. In the first case, indicated as *distance-based* selection, the close approaches are chosen considering their distance from the celestial body, which may or may not be normalised by the radius of the sphere of influence of the planet. In the second case, called *state-based* selection, the identification of the *worst* close encounter depends on the state of the trajectory (e.g. simple close approach, resonance, impact) and on the celestial body involved in the encounter. This approach is particularly suitable for the application to planetary protection as the planets have different requirements. When using this approach, the user can provide a list of *priority* of the celestial bodies (e.g. events with Mars are more important than the ones with Mercury) to ensure that the close approaches with specific celestial bodies are highlighted.

3. RESULTS

The method was applied to verify the compliance of a mission considering two scenarios: in the first case, the dispersion of the initial condition due to the inaccuracy of the launcher is considered; in the second case, the dispersion derives from potential failures of the propulsion system on the spacecraft. Two applications belonging to the first scenario are discussed in [16], where the compliance with planetary protection requirements is studied for the launcher of Gaia and the one of BepiColombo. In the following, the case of the launcher of Solo will be presented, together with the study of the failure of the propulsion system of BepiColombo.

3.1. Dispersion of the launcher

For the first application, the dispersion of the initial condition of Solo is studied with the approach presented in Section 2. The covariance matrix associated with the initial state vector of the launcher is used to generate the dispersion of position and velocity. The parameters of the simulations are reported in Table 1. A test with 1000 MC runs was performed; the effect of solar radiation pressure is not considered.

Figure 7 shows the dispersion of the MC runs in terms of the deviation from the initial nominal velocity: Δv_a indicates the velocity deviation in the along-track direction and Δv_r the deviation in the radial direction. Each dot corresponds to one MC run and the colour depends on the classification based on the *worst* close approach. It is interesting to observe how the trajectory of the launcher of Solo can interact with three different celestial bodies. The vast majority of the cases (989) enters in the sphere of influence of Venus, with 266 cases of resonances and 51 impacts. A few cases (10) result into resonances with the Earth and one case in a close approach with Mars. As in previous results obtained for the launcher of BepiColombo [16], the different trajectory states appear as bands in the diagram of the velocity dispersion.

The distribution of the close approaches with Venus on its b-plane is shown in Figure 8. For the launcher of Solo, the trajectories go *directly* to Venus, differently from the case of the launcher of BepiColombo, where a fly-by of the Earth was re-

Table 1: Parameters for the simulation of the dispersion of the launcher of Solo.

Number of MC runs	1000
Number of impacts	51 (Venus)
Propagation length	100 years
Propagator	RK8(7)
Ephemeris	Improved ESA routine
Computational time	17 minutes
When multiple CA	<i>worst</i> case
<i>Worst</i> definition	state-based

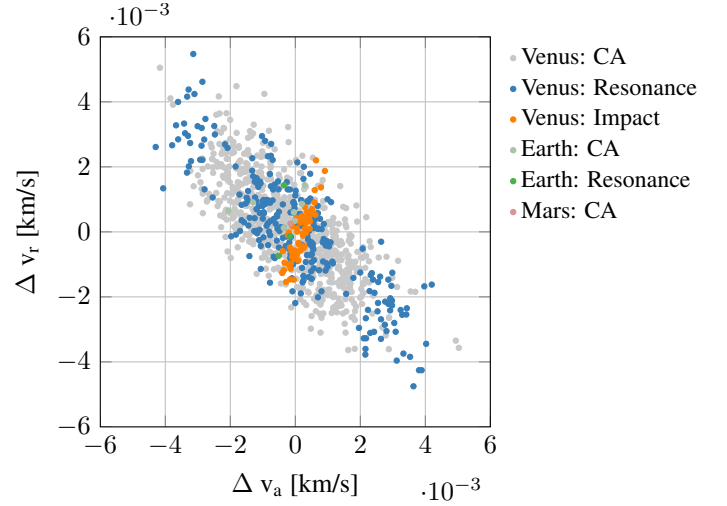


Fig. 7: Velocity dispersion and trajectory characterisation for the Monte Carlo analysis on the launcher for Solo. CA indicate a *close approach*. Δv_a is the velocity deviation in the along-track direction, Δv_r is the velocity deviation in the radial direction.

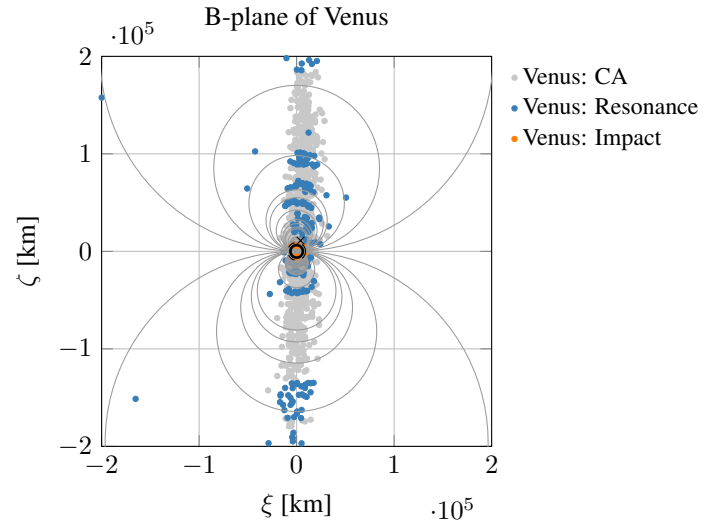


Fig. 8: Representation of the worst close approaches for the 1000 Monte Carlo runs of the launcher of Solo on the b-plane of Venus.

sponsible for the entrance in the sphere of influence of Venus [16]. From Figure 8 it appears how the dispersion of the initial state affects mostly the phasing between the launcher and the planet (variation of the coordinate ζ).

3.2. Failure of the propulsion system

In this second application, the failure of the propulsion system of BepiColombo is studied, considering potential failures of the propulsion system during the Earth-to-Earth arc. The trajectory is provided to the program as an input text file. SNAPSHOT generates random failure time instants within the thrust arcs. The state vector associated to the failure time is obtained by linear interpolation of the state vector between the two closest times. The parameters of the simulations are reported in Table 2. The number of 54114 corresponds to the verification of the planetary protection requirement of a probability of impact with the reference body (Mars) lower than 10^{-4} , with a confidence level equal to 99%. In total, 28 impacts with the Earth were found.

Figure 9 shows the summary of the Monte Carlo analysis, representing for each run the coordinates of the *worst* close encounter on the b-plane of the Earth, so the points may refer to different time of close approach. The blue points represent conditions of impact: as explained, they are found also at distances larger than the radius of the Earth, indicated in the figure by the thick black line, because all the points within the *impact region* defined in Section 2 result in impacts. The light blue points indicate conditions of resonance and 6542 runs belongs to this category. Finally, dark grey points represent simple close approaches, i.e. all the cases where the spacecraft enters the sphere of influence of the Earth. This happens for more than 35% of the simulated cases (including the ones that result in impacts and resonances). Looking at Figure 9 one can notice how the points are distributed along a distinct vertical line (and some less defined ones). These lines corresponds to close approaches with similar conditions at the entrance of the sphere of influence, with only a variation in the phasing between the spacecraft and the Earth.

Figure 10 shows the distribution of resonances and impacts with the failure time and the minimum distance from

Table 2: Parameters for the simulation of the failure of the propulsion system of BepiColombo.

Number of MC runs	54114
Number of impacts	28 (Earth)
Propagation length	100 years
Propagator	RK8(7)
Ephemeris	Improved ESA routine
Computational time	104 minutes
When multiple CA	<i>worst</i> case
<i>Worst</i> definition	state-based

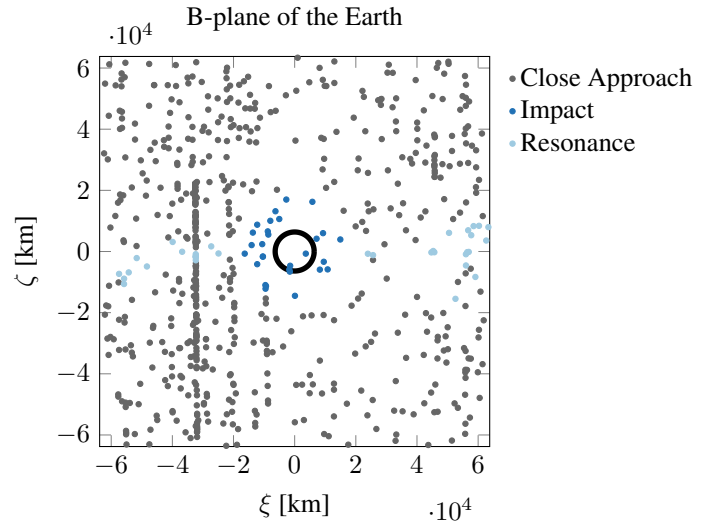


Fig. 9: Worst close approaches of BepiColombo represented on the b-plane of the Earth.

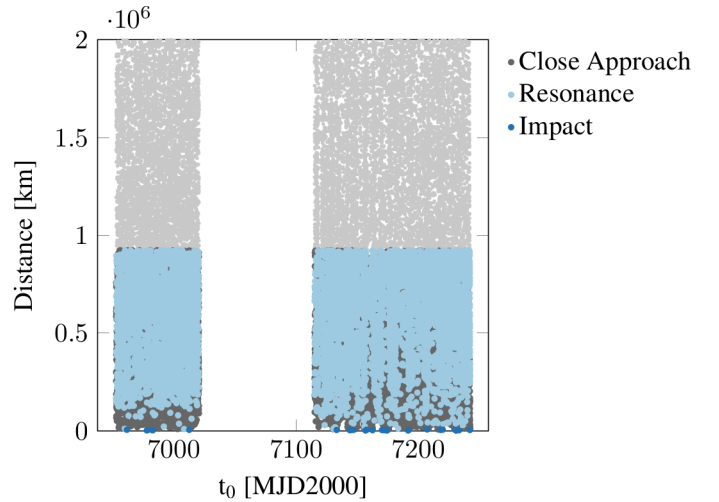


Fig. 10: Close approach state represented as a function of the time of failure and of the distance from the Earth. Thrust arcs extend from 6953 to 7021 and from 7115 to 7242.

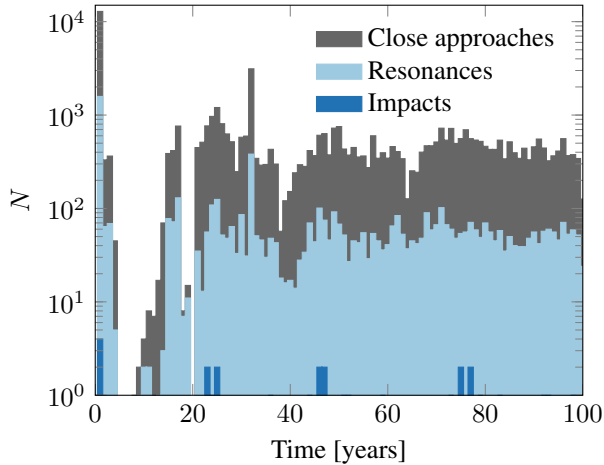


Fig. 11: Distribution of the time of worst close approach for the failure of BepiColombo propulsion system. The time 0 refers to the epoch 6953 MJD2000.

the Earth. Focussing on the dark blue dots on the x -axis, one can notice how failures in both the considered thrust arcs may result into impacts with the Earth. Moreover, the probability of impact and resonances seems the same for failures in both thrust arcs.

Finally, Figure 11 shows the distribution of the time of the worst close approach, considering as origin of the x -axis the epoch of the first point of the first thrust arc (6953 MJD2000). The two thrust arcs cover a period of nine months and a half; failures from both arcs contribute to the peak in Figure 11 between one and two years after the reference epoch. The peak contains more than 12000 cases.

4. CONCLUSIONS

The compliance with planetary protection requirements needs to be verified for all interplanetary missions and missions to the Lagrangian points as the spacecraft and the launchers used for these applications may be inserted into trajectories that can impact a celestial body. The requirements are usually defined in terms of a maximum allowed impact probability over 50-100 years and they should be verified considering possible inaccuracies in the launch system or failures on the spacecraft.

A new tool, SNAPSHOT, was developed for this purpose: it is based on a Monte Carlo approach and the representation of close encounters on the b -plane. The simulation is initialised by setting the maximum allowed impact probability and the desired confidence level. From these two parameters, the number of runs necessary to verify the requirement is derived and increased if impacts with a reference celestial body are detected. The method can be applied to study the dispersion of the launcher, as described by covariance matrix, or the failure of the propulsion system, generating random failure times. In both cases, additional distributions, such as

the one of the area-to-mass ratio, may be considered.

Each initial condition is propagated using a Runge-Kutta method. The effect of gravitational forces and of the solar radiation pressure is considered. Three options are available for the ephemerides of the celestial body, among which the ESA routine proved to be the fastest. Several integrators based on Runge-Kutta methods are available, together with two main techniques for the control of the step-size. The first one is the traditional adaptive technique, the second, called *regularised* steps, scales the steps according to the evolution of the dynamics.

Once the trajectory is obtained, it is analysed to detect close approaches with celestial bodies. The entrance in the sphere of influence of a body is used as the definition of a close approach and, under this condition, the representation on the b -plane is used. This enables the identification of impacts and resonances with a celestial body. If along a trajectory more close approaches are registered, the first one or the *worst* can be used to define the output of the MC run. In the latter case, the *worst* close approach can be defined as the one with the minimum distance from a celestial body or as the most critical one depending on the state of the trajectory (e.g. resonances) and the involved celestial body.

SNAPSHOT was applied to study two cases: the evolution of the trajectory of the launcher of Solo and the failure of the propulsion system of BepiColombo. In the first case, it was found that the trajectory of the launcher can interact with Venus, Earth, and Mars. The distribution of the different trajectory state with the initial velocity deviation shows the presence of bands corresponding to specific states (e.g. impacts with Venus). In the second case, the failure of the propulsion system of BepiColombo was studied. 54114 Monte Carlo runs were performed to demonstrate that the probability of impact with the reference planet (Mars) is below 10^{-4} , with a confidence level equal to 99%. Whereas no impacts with Mars were detected, 28 impacts with the Earth were registered, originating from failures in both the studied thrust arcs.

The propagation for 100 years and the trajectory analysis require around 1 s for each Monte Carlo run in the case of the launcher of Solo and even less for the case of BepiColombo. For this reason, this approach appears suitable for the study of a large number of samples. A similar approach could be extended to the study of robust manoeuvre design and to the one of deflection strategies for asteroids.

References

- [1] R. Jehn, "Estimating the impact probability of ariane upper stages," European Space Agency, Tech. Rep. MAS Working Paper 601, Dec. 2014.
- [2] ESA Space Debris Office, "Reentry data will help improve prediction models," Oct. 2015, accessed 14 January 2016. [Online].

Available: http://www.esa.int/Our_Activities/Operations/Space_Situational_Awareness/Reentry_data_will_help_improve_prediction_models

- [3] G. Kminek, "Esa planetary protection requirements," European Space Agency, Tech. Rep. ESSB-ST-U-001, Feb. 2012.
- [4] R. Jehn, "Estimation of impact probabilities of interplanetary ariane upper stages," in *30th International Symposium on Space Technology and Science*, Jul. 2015.
- [5] M. S. Wallace, "A massively parallel bayesian approach to planetary protection trajectory analysis and design," in *AAS/AIAA Astrodynamics Specialist Conference*, Aug. 2015.
- [6] A. DasGupta, *Asymptotic Theory of Statistics and Probability*, ser. Springer Texts in Statistics. Springer New York, 2008.
- [7] J. Monahan, *Numerical Methods of Statistics*, ser. Cambridge Series in Statistical and Probabilistic Mathematics. Cambridge University Press, 2001, no. v. 1.
- [8] P. Dysli, "Analytical ephemeris for planets," 1977.
- [9] J. Dormand and P. Prince, "A family of embedded runge-kutta formulae," *Journal of Computational and Applied Mathematics*, vol. 6, no. 1, pp. 19 – 26, 1980. [Online]. Available: <http://www.sciencedirect.com/science/article/pii/0771050X80900133>
- [10] F. Debatin, A. Tilgner, and F. Hechler, "Fast numerical integration of interplanetary orbits," in *Second International Symposium on Spacecraft Flight Dynamics*. European Space Agency, Oct. 1986.
- [11] D. Sarafyan, "Robust and reliable defect control for runge-kutta methods," *ACM Transactions on Mathematical Software*, vol. 33, no. 1, 2007. [Online]. Available: <https://focus.library.utoronto.ca/works/9291>
- [12] L. Shampine, "Interpolation for variable order, runge-kutta methods," *Computers & Mathematics with Applications*, vol. 14, no. 4, pp. 255 – 260, 1987. [Online]. Available: <http://www.sciencedirect.com/science/article/pii/0898122187901337>
- [13] J. Davis, P. Singla, and J. Junkins, "Identifying near-term missions and impact keyholes for asteroid 99942 apophis," in *7th Cranfield Conference on Dynamics and Control of Systems and Structures in Space*, 2006.
- [14] E. Öpik, *Interplanetary encounters: close-range gravitational interactions*, ser. Developments in solar system and space science. Elsevier Scientific Pub. Co., 1976.
- [15] G. B. Valsecchi, A. Milani, G. F. Gronchi, and S. R. Chesley, "Resonant returns to close approaches: Analytical theory," *Astronomy & Astrophysics*, vol. 408, no. 3, pp. 1179–1196, 2003. [Online]. Available: <http://dx.doi.org/10.1051/0004-6361:20031039>
- [16] F. Letizia, C. Colombo, J. P. J. P. Van den Eynde, and R. Jehn, "B-plane visualisation tool for uncertainty evaluation," in *26th AAS/AIAA Space Flight Mechanics Meeting*, Feb. 2016.